Exploring the role of lignin structure in molecular dynamics of lignin/bio-derived thermoplastic elastomer polyurethane blends

P. Ortiz-Serna[a], *M. Carsi*[b,*], *M. Culebras*[c], *M. N. Collins*[c] *and M. J. Sanchis*[a,*]

[a]Department of Applied Thermodynamics and Institute of Electric Technology, Universitat Politècnica de València, Camino de Vera s/n, Valencia, 46022, Spain.

[b]Department of Applied Thermodynamics and Instituto de Automática e Informática Industrial, Universitat Politècnica de València, Camino de Vera s/n, Valencia, 46022, Spain.

[c]Stokes Laboratories, Bernal Institute, School of Engineering, University of Limerick, Ireland.

*Corresponding authors.

E-mail addresses: jsanchis@ter.upv.es (M. J. Sanchis), mcarsi@ai2.upv.es (M. Carsí).

ABSTRACT

The relaxation behavior of two lignins (Alcell organosolv, OSL, and hydroxypropyl modified Kraft, ML) and bio-based thermoplastic polyurethane (TPU) blends have been studied by Differential Scanning Calorimetry (DSC), Dynamic-Mechanical Analysis (DMA) and Dielectric Relaxation Spectroscopy (DRS). The effect of blending on the glass and local relaxation

processes as a function of composition, frequency, and temperature has been assessed. The dielectric spectra were resolved into dipolar relaxations as well as conductive processes for differing blend compositions. Characteristic relaxation times, activation energies and dielectric relaxation strengths of lignin/*x*TPU blends were also investigated. It was found that blending suppresses the α-relaxation process of the blends compared to virgin TPU. On the other hand, while the position of the β-relaxation was not influenced by blending, a reduction of the activation energies, E_a, of this process was observed in the lignin/*x*TPU blends. Finally, changes are observed in the conductivity behavior of both blends, with conductivity processes more favorable for the OSL/*x*TPU blends.

KEYWORDS: Bio-based blends, lignin, thermoplastic elastomeric polyurethane, relaxation behavior, thermal analysis.

1. Introduction

Sustainable development of materials is one of the biggest global challenges facing society [1,2]. Ever increasing amounts of CO_2 emission coupled with the inherent depletion of oil-based resources, creates the necessity to find alternative sources to synthesize novel materials, in particular, polymer and carbon based compounds [3-5]. The valorization of lignocellulose biomass is showing great potential as a renewable source for raw materials with the potential to develop high value products such as: porous carbon materials [6], 2,5-Furandicarboxylic acid [7, 8], furfural [9] and 5-Hydroxymethylfurfural [10]. It is widely available and not in competition with food based crops [11,12]. Lignocellulose biomass is composed mainly of three components: cellulose, hemicellulose, and lignin. Cellulose is widely used in the paper and textile industries

while hemicellulose is a source of C_5 and C_6 used to produce valuable chemical compounds for the production of biofuels [13]. However, lignin is a low value by-product without a well-defined application. Generally, only 2% of lignin is isolated from cellulose in the paper and pulp industry, and this is currently finding use in some low value applications such: soil, activated carbon or fertilizers. The remaining lignin is burned on site as an energy source [14,15]. Therefore, it is of major scientific, environmental and social importance to find new technological processes that can valorize lignin in order to use lignin biomass efficiently, replace unsustainable petroleum-based materials and achieve a zero waste society. An application that has shown enormous potential for lignin is the manufacture of carbon fibers [16-20]. However, the technological development of this area is not mature enough to be exploited commercially due to several problems associated with lignin processability namely: brittleness, slow stabilization processes and difficulties to achieve a good carbon phase during the carbonization [21]. To overcome these issues, it has become apparent that the blending of lignin with compatible biopolymers is highly attractive [18]. In order to determine optimized blends, it is essential to have a clear understanding of the underlying physical and chemical properties associated with each of the blended materials. Through careful selection of the blended components, the ratio between them and their processing method, it is possible to tailor the processing properties of the polymer blends. Very few polymers are completely miscible with lignin, poly(ethylene oxide) (PEO) [22,23], polyethylene terephthalate (PET) [24] and poly(N-vinylpyrrolidone) (PVP) [25] are the most well-known. However, recently we have discovered that bio-based segmented thermoplastic elastomeric polyurethanes are compatible with lignin [26], resulting in improved mechanical properties whilst allowing lignin to be processed into, for example, carbon fibers [27]. However, in order to gain further insights into the mechanism

involved, it is necessary to provide a complete understanding of the molecular interactions between these two polymers to optimize their processability and mechanical properties. Miscibility depends on the molecular structure of the polymer components, on their morphologies, on their blend composition, and their Flory-Huggins interaction parameters as well as processing conditions. Miscibility is enhanced through the introduction of strong intermolecular interactions, e.g. hydrogen bonding, dipole-dipole, and ionic interactions [28,29]. Several techniques can be used to understand specific interactions in polymers. Here, we use Dielectric Relaxation Spectroscopy (DRS) [30] to obtain a complete understanding of the molecular dynamics and the nature of interactions in polymer blends produced from lignin and a bio-based thermoplastic polyurethane, through the monitoring of the motion of dipolar groups attached to molecular chains. In addition, complementary DSC and DMA measurements were carried out in order to provide information about the degree of miscibility of the blends [31].

2. Experimental

2.1. Materials

Thermoplastic polyurethane (TPU), Pearlthane ECO 12T95, was synthesized from castor oil, methylene diphenyl diisocyanate and 1,4-butanediol, according to manufacturing information provided by Lubriozol (Veltox, France). A simplified schematic chemical structure of the TPU precursors is reported in Scheme 1. Alcell organosolv hardwood lignin (OSL) with a M_w of 4000 g mol^{-1} (phenolic content 2.4 mmol g^{-1}) and hydroxypropyl modified Kraft hardwood (ML) with a M_w of 11400 g mol^{-1} (phenolic content 0.33 mmol g^{-1}) were obtained from Tecnaro GmbH (Germany). The simplified molecular structures of both lignins are shown in Scheme 2.

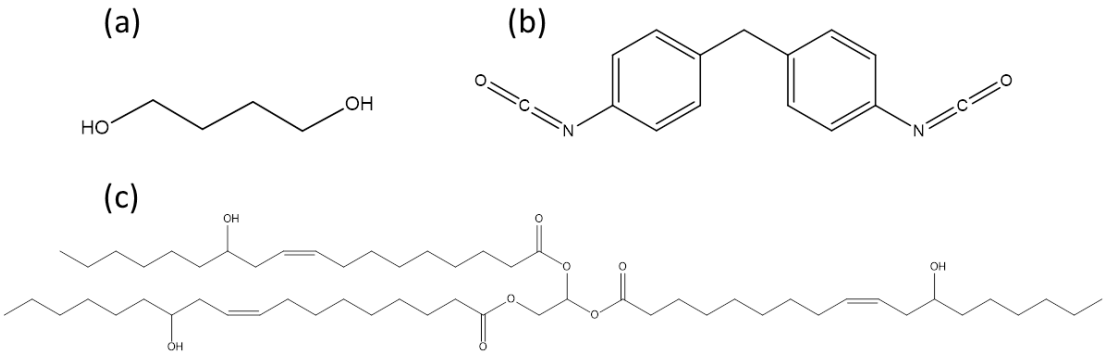

Scheme 1. Molecular structure of TPU precursors. (a) 1,4-butanediol, (b) methylene diphenyl diisocyanate and (c) castor oil.

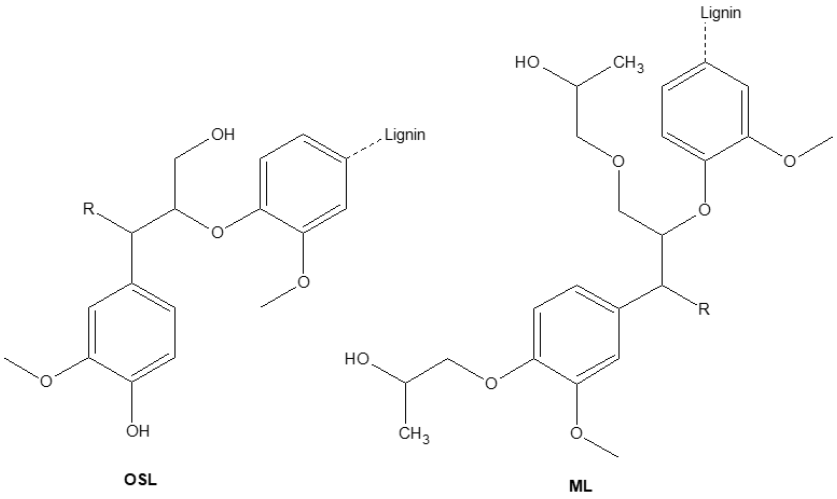

Scheme 2. Simplified lignin molecular structures used in this study.

2.2. Synthesis of Lignin/xTPU Blends

Samples were extruded twice using a Xplore MC15 microcompounder. Materials were compounded during the first run and the second run was used to produce the films. The die dimensions were 1.5 mm for compounding and (40×1) mm for the film production. The screw speed was 100 rpm for compounding and 50 rpm for fiber spinning. All prepared samples and

the temperature profile used are summarized in Table 1. The ML/30TPU blend exhibited brittleness when handled and this has been attributed to the higher branching degree of ML [26].

Table 1

Composition and nomenclature of the blends analysed.

	%wt TPU	% *wt* OSL	% *wt* ML	Processing temperature (K)
TPU	100	—	—	428/453/463/463
OSL/30TPU	30	70		428/453/463/453
OSL/40TPU	40	60		428/453/463/453
OSL/50TPU	50	50		428/453/463/453
ML/30TPU	30		70	448/463/473/463
ML/40TPU	40		60	448/463/473/463
ML/50TPU	50		50	448/463/473/463

2.3. Differential Scanning Calorimetry (DSC) measurements

Differential Scanning Calorimetry (DSC) measurements were performed using a TA Instrument Q20 (USA) equipped with a refrigerated cooling system. The DSC tests were performed under a 50 mL min^{-1} flow of N_2 to prevent oxidation. Calibration was undertaken with indium in accordance with manufacturer specifications. Thin films were repeatedly stacked onto a pan, to achieve a weight of approximately 8-12 mg. Measurements were conducted in crimpled non-hermetic aluminum pans. Scans were performed from 193 to 423 K (TPU), from 318 to 427 K (lignins) and from 193 to 433 K (lignin/*x*TPU blends) at a heating rate of 20 K min^{-1}. Glass

transition temperatures (T_g) were evaluated as the middle point of the heat capacity change on the second heating run.

2.4. Dynamic-Mechanical Analysis (DMA) measurements

Dynamic-Mechanical measurements were carried out using a DMA Q800 from TA Instruments (USA). Oscillatory tests at a frequency of 1 Hz were performed in tensile mode with an amplitude of 10 μm. Samples were pre-treated in an oven at 313 K for at least 24 h to prevent the influence of humidity. Test specimens with a dimension of 40×5×(0.3-0.4) mm^3 were cut from the prepared films. The dynamic modulus E^* was measured in the range from 173 K to 428 K, at a heating rate of 3 K min^{-1} under the nitrogen atmosphere. The storage modulus (E'), loss modulus (E'') and loss tangent ($\tan \delta = E''/E'$) were recorded as a function of temperature.

2.5. Dielectric Relaxation Spectroscopy (DRS) measurements

The Dielectric measurements were conducted employing a Novocontrol Broadband Dielectric Spectrometer (Hundsagen, Germany) consisting of an Alpha analyzer to carry out measurements in the frequency range from 5×10^{-2} to 3×10^{6} Hz. The temperature was controlled by a Novocontrol Quatro cryosystem, with a precision of ±0.1 K during each frequency sweep. Molded disc shaped samples of 20 mm diameter and 0.17-0.52 mm thickness were mounted in the dielectric cell between two parallel gold-plated electrodes. The thickness of each sample was measured with a micrometer. Before every measurement, samples were dried at 313 K, in a vacuum oven until constant weight to avoid interference of water in the dielectric response. In addition, a measurement was made at 373 K, for all samples, before the programmed temperature sweep to ensure moisture elimination. Isothermal measurements were performed in an inert N_2 atmosphere, from 153 K to 393 K, 408 K and 423 K, depending on the blend, with a

step of 5 K, to avoid moisture uptake. These temperature ranges were chosen in order to cover the glass transition temperatures. The experimental uncertainty was less than 5% in all cases.

3. Results and discussion

3.1. Differential Scanning Calorimetry (DSC) measurements

Fig. 1 shows the DSC thermograms of the synthesized blends, as well as their polymer constituents. For TPU, microphase separation occurs upon cooling from the melt, which results in the formation of hard and soft domains [32]. Thus, TPU displays two endothermic processes. Lower temperature transitions are associated with the T_g of soft segments (239.5 K) corresponding to the molecular motion of alkyl chain groups of castor oil based polyols. Higher temperature transitions are associated with hard segments (293.8 K), attributed to the molecular motion of rigid components [33]. In the case of OSL blends the absence of this peak indicates the lack of interactions between the hard segments of TPU since they interact with Lignin segments via H-bonding [27]. However, in the case of ML blends this peak is present indicating that there are interactions between the hard segments of TPU chains. Therefore, the molecular structure of ML is not suitable to establish intermolecular interactions with the hard segments of TPU.

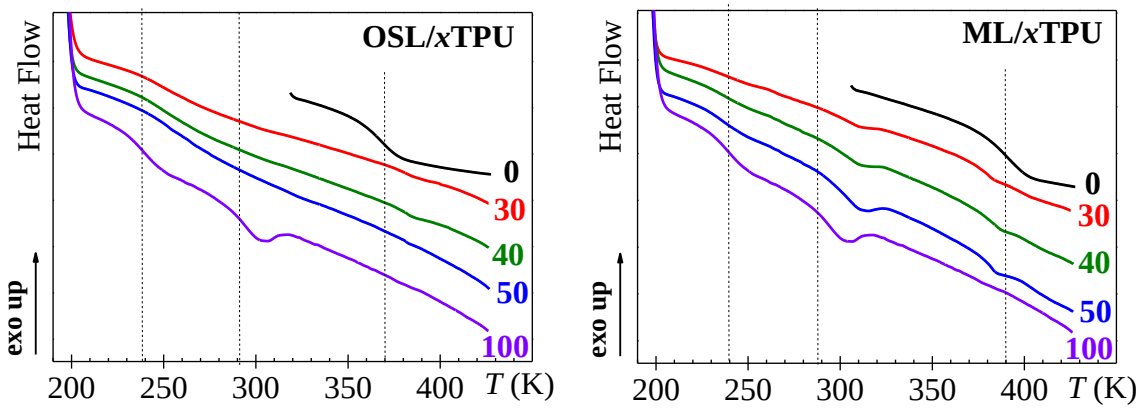

Fig. 1. DSC experimental curves for OSL/*x*TPU and ML/*x*TPU samples (*x*= 0, 30, 40, 50 and 100). Data are vertically shifted for better visualization. The dashed lines correspond to the TPU homopolymer and lignins T_g's.

Table 2 shows a clear visualization of the T_g tendency of polymer blends as a function of composition. Taking OSL and ML lignins, endothermic transitions associated with the glass transition of each lignin were recorded at 369.8 K and 383.7 K, respectively [27]. On the other hand, lignin/*x*TPU blends show complex DSC thermograms due to the overlapping of the different glass transitions observed: soft and hard segments of the TPU and lignin (OSL or ML), which complicates the identification of these processes.

Table 2

Glass transition of the TPU homopolymer, lignins and lignin/*x*TPU blends.

	% TPU	0	30	40	50	100
OSL/*x*TPU	T_g^{OSL}(K)	369.8	381.8	381.9	383.2	—
	$T_g^{soft\ TPU}$(K)	—	248.5	269.5	276.1	239.5
	$T_g^{hard\ TPU}$(K)	—	286.8	—	—	293.8
ML/*x*TPU	T_g^{ML}(K)	383.7	382.0	382.6	382.7	—
	$T_g^{soft\ TPU}$(K)	—	240.8	237.7	235.2	239.5
	$T_g^{hard\ TPU}$(K)		304.5	305.1	305	293.8

Thus, for OSL/*x*TPU blends with percentages greater than 30% of TPU, a single broad glass transition is observed, presumably due to hydrogen bond formation between TPU chains and

OSL at these levels [27]. Due to the complexity in identifying the T_g's in OSL/*x*TPU blends, miscibility/immiscibility cannot be conclusively determined by DSC. However, from the thermograms, initial deviations from the baselines are associated with the onset of the T_g of TPU soft segments. For OSL/*x*TPU blends, a higher value of T_g is observed for all the compositions when comparing with the TPU itself, suggesting a decrease of molecular mobility of TPU chains upon blending. Nevertheless, the T_g of TPU soft segments decreases with OSL content. This trend is attributed to the higher free volume available in the blends with lower TPU content. The second deviation is associated with the T_g of the hard segments of TPU and this vanishes as the OSL content decreases. This behavior is presumably due to the chemical interactions associated with hydrogen bonding between the lignin and the TPU that hinder the mobility of the hard segments. Finally, the T_g of OSL lignin, increases with the TPU content, which is attributed to the intensification of molecular packing as blending is increased, presumably due to the presence of hydrogen bonding and π stacking between OSL and TPU.

For ML/*x*TPU blends, the individual T_g's, in all compositions, analyzed are visible. A slight decrease of T_g is observed for ML/40TPU and ML/50TPU blends when comparing with the TPU, suggesting an increase of molecular mobility with blending. On the other hand, the T_g's associated with hard segments of TPU and blended with ML remain unchanged.

Blending OSL lignin with TPU produces an increase of approximately 12 K in the T_g of OSL lignin. This increase is most probably due to the chemical structure of OSL which favours the formation of hydrogen-bonding with TPU as a result of its higher phenolic content and lower molecular weight.

On the other hand, blending ML lignin with TPU produces a decrease of only 1-2 K in the T_g of ML lignin. In this case, ML displays less hydrogen bonding than OSL due to its higher branching degree and longer chains [27]. Therefore, TPU plays a plasticizing effect that improves processability, flowability, and extensibility of these blends.

3.2. Dynamic Mechanical measurements

Fig. 2 shows the temperature dependence of the mechanical modulus (a and b) and loss modulus (c and d) for TPU and lignin/*x*TPU blends at 1 Hz. The DMA spectra of both families of blends show similarities, but also differences in shape and height.

The storage modulus values decrease with increasing temperature, but this reduction occurs at higher temperatures for blends with lower OSL lignin content (Fig. 2a). This tendency agrees with the DSC results. For ML/*x*TPU blends, the temperature dependence of the storage modulus (Fig. 2b) is different, especially for ML/30TPU blend, presumably due to the crosslinking interactions than occur in ML lignin, which increase the blend rigidity.

For both lignin/*x*TPU blends, two overlapping relaxation processes, related to the TPU homopolymer T_g's and a secondary relaxation process, are observed in the E'' temperature dependence spectra (Fig. 2c and 2d). However, for high temperature processes, there are noticeable differences between the blends, both in the position and in the broadness of the responses. Taking the homopolymer TPU as reference, a large displacement towards higher temperatures is observed in the blends with OSL, whilst peak broadness remains nearly constant (see inset in Fig. 2c). On the other hand, for ML/*x*TPU blends the maximum temperature does not change, while the broadness of the peak increases with increasing ML content (see inset in Fig. 2d). These trends correlate well with DSC results.

For low temperature processes (secondary relaxation) a decrease in intensity is observed with the incorporation of OSL lignin, in contrast, for ML/*x*TPU blends an opposite tendency is observed. These trends are related to the decrease and increase of the molecular mobility of the TPU units responsible for this process, respectively. The peak at circa 390K of ML/30TPU is attributed to crosslinking reactions between ML chains and this causes a viscoelastic response.

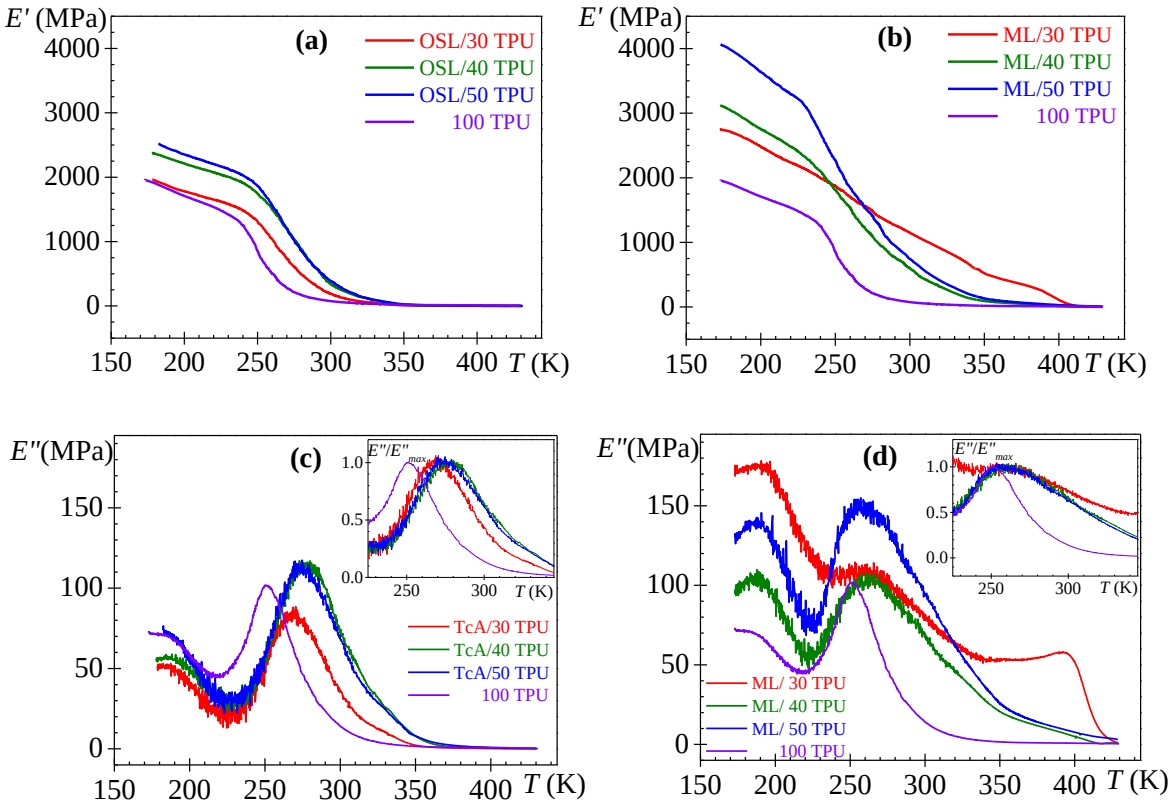

Fig. 2. Temperature dependence of *E′* and *E″* at 1 Hz for TPU and lignin/*x*TPU blends.

3.3. Dielectric Relaxation Spectroscopy (DRS) measurements

Fig. 3 and 4 show temperature dependence of the permittivity constant and loss permittivity of TPU and blends at two characteristic frequencies (1.19 and 10^3 Hz). At 1.19 Hz, the temperature

dependence of ε′ for TPU shows a broad transition between 223 to 323 K, possibly as a result of the overlapping of the glass transitions associated with the soft and hard segments of TPU. As temperature increases, other transitions associated with interfacial polarization processes are observed [32,34]. Interfacial polarization processes are especially dominant at high temperature and low frequencies, often masking the dipolar processes. Similar trends are presented for the two lignin/*x*TPU blends, with two interfacial polarization processes observed. The first one is labeled as the Maxwell-Wagner-Sillars (MWS) process, which is the result of the separation of charges at internal phase boundaries for heterogeneous blends [34-36]. The MWS process follows a sharp rise in permittivity at higher temperatures related to the electrode polarization (EP) process, which takes into account the conduction process at the polymer-electrode interface [37].

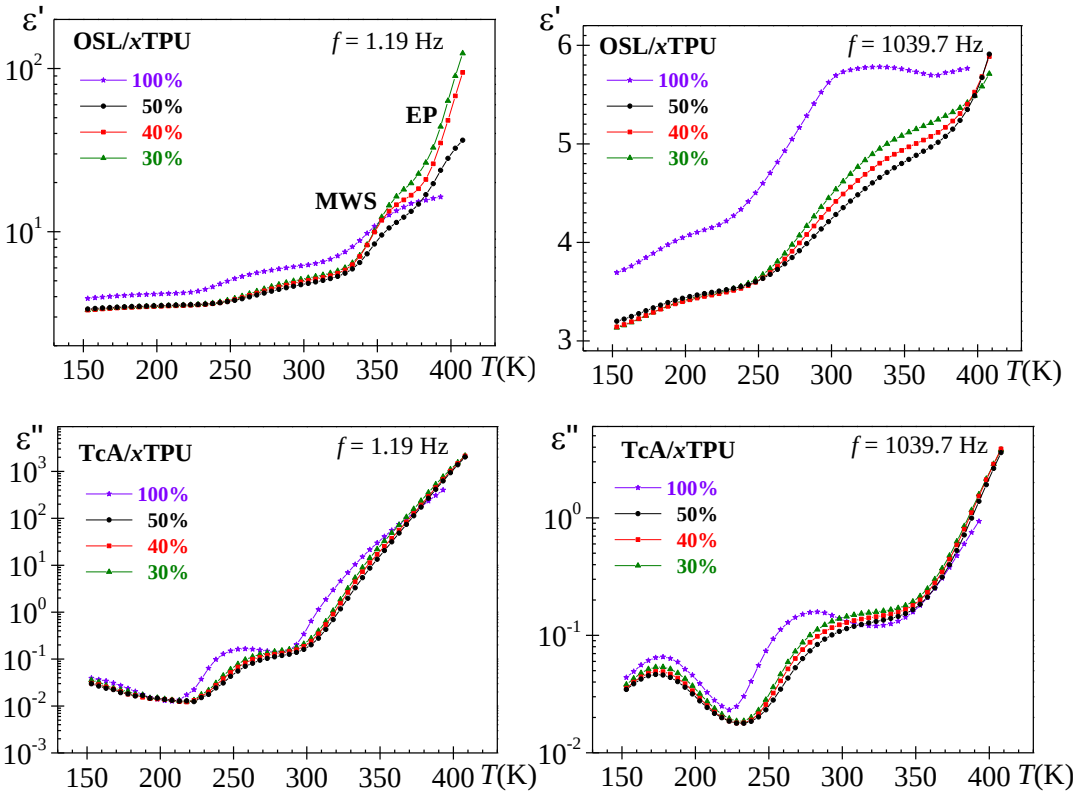

Fig. 3. Temperature dependence of ε′ (top) and ε″ (bottom) at 1.19 and 1039.7 Hz for the OSL/*x*TPU blends (*x* = 30, 40, 50 and 100).

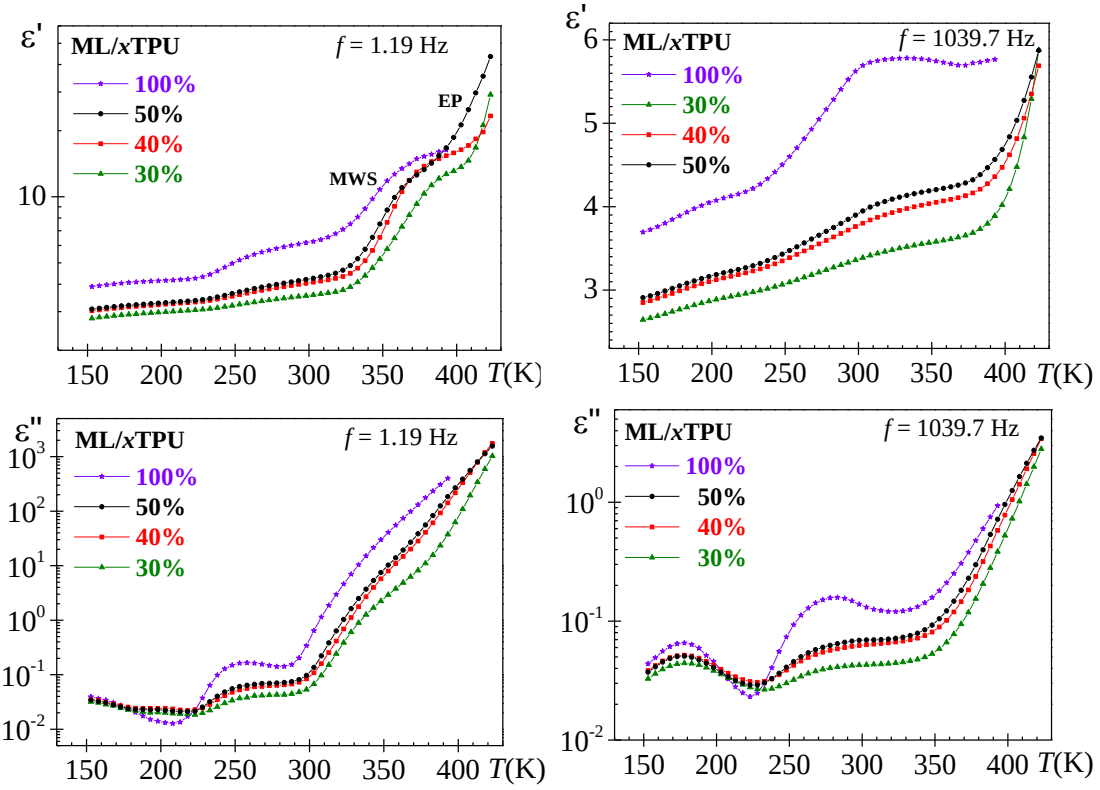

Fig. 4. Temperature dependence of ε′ (top) and ε″(bottom) at 1.19 and 1039.7 Hz for the ML/*x*TPU blends (x = 30, 40, 50 and 100).

Fig. 3 and 4 also show two dipolar relaxation processes in the loss permittivity spectra for both TPU and TPU/lignins. In order to better visualize the influence of lignin chemistry on the

position and height of both dipolar processes, the temperature dependence of ε″ for TPU and for lignin/40TPU blends has been plotted in Fig. 5. While the position of the low temperature process is not significantly affected by the type of lignin, a notable difference is observed in the high temperature process, related to the vitreous transition (soft and hard segments) of the TPU. The low temperature process, labeled as β-relaxation, is related to the molecular motion of TPU units with restricted mobility. Both, the position and the height of this secondary dipolar process of TPU are slightly affected, with the height most affected in all cases. On the other hand, for the high temperature dipolar process in the OSL/*x*TPU blends, a small decrease in height with a shift to higher temperatures is observed with respect to TPU. For the ML/*x*TPU blend, the process position is not appreciably affected by the incorporation of ML, however, the process height is significantly reduced. With increasing temperature, a sharp increase in dielectric loss is observed, and this is attributed to the dielectric response of lignin and/or with the presence of conductive processes.

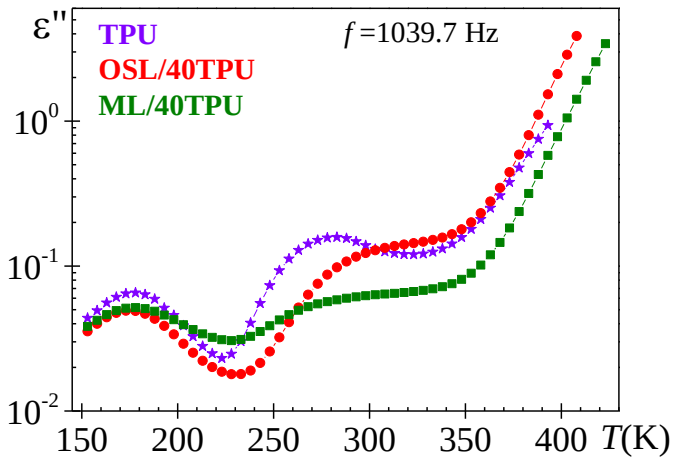

Fig. 5. Temperature dependence of dielectric loss permittivity of TPU and lignin/40 TPU (lignin = OSL and ML) at 1039.7 Hz.

In order to obtain a better definition of the high temperature processes [38], the temperature dependence of the dielectric loss modulus, M'', has been represented in Fig. 6. Unfortunately, this alternative representation does not allow a clear view of the glass transition processes due to the overlapping of relaxation processes with conduction phenomena. For TPU at approximately 333 K a defined conductive process, not well-defined in the ε'', is observed. In the case of OSL/*x*TPU blends, the position and broadness of this peak remain practically unchanged. On the other hand, for ML/*x*TPU blends, this process is clearly overlapped with another one, presumably associated with the glass transition temperature of the ML lignin, which induces changes in the position and broadness of the peak.

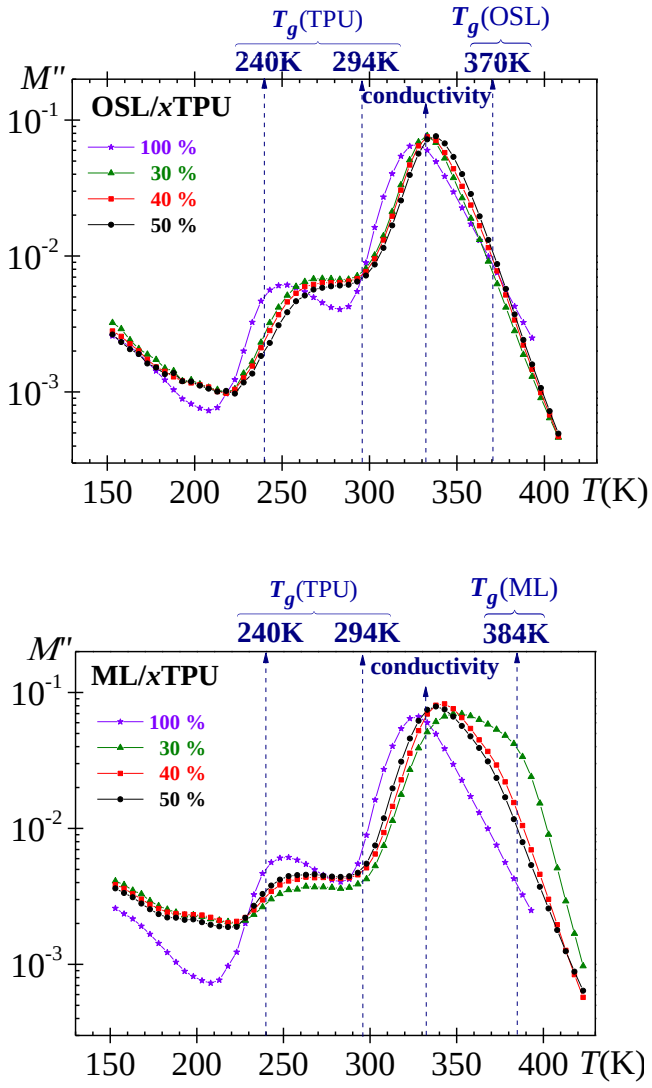

Fig. 6. Temperature dependence of loss dielectric modulus, *M″*, for TPU and lignin/*x*TPU blends (*x* = 30, 40, 50 and 100 and lignin = OSL and ML) at 1.19 Hz. The glass transition temperatures of the homopolymers obtained by DSC are included in the top of the figures.

Fig. 7 shows isotherms between 153 K and 223 K for the dielectric loss of TPU and lignin/*x*TPU blends. Analysis of the dielectric spectra was performed utilizing the empirical equation of Havriliak-Negami (HN) [39-41], which relates the complex permittivity (ε^*) to the frequency by

$$\varepsilon^*_{dip}(\omega) = \varepsilon_\infty + \frac{\varepsilon_0 - \varepsilon_\infty}{\left[1+\left(j\omega\tau\right)^{a_{HN}}\right]^{b_{HN}}} \quad (1)$$

where τ is the relaxation time of the process, $\omega = 2\pi f$ is the angular frequency and the subscripts ε_0 and ε_∞ are, respectively, the relaxed ($\omega = 0$) and unrelaxed ($\omega = \infty$) dielectric permittivity. The dielectric strength relaxation, defined as $\Delta\varepsilon = \varepsilon_0 - \varepsilon_\infty$, is related to both, the dipole moment and the number of entities that participate in the relaxation process. The shape parameters a_{HN} and b_{HN} must fulfill the condition $0 < a_{HN}, b_{HN} \leq 1$, being $a_{HN} = b_{HN} = 1$ for a Debye process. The a_{HN} parameter is related to the peak broadness, the higher the a_{HN} parameter the narrower the peak is. The b_{HN} parameter is related to the skewness of the plot along a straight line at high frequencies. For secondary absorptions, the b_{HN} parameter is equal to one.

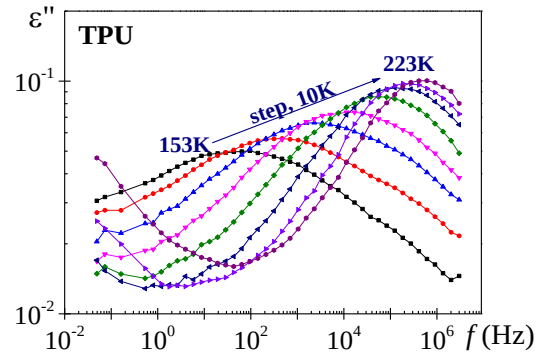
ε''
TPU
223K
step, 10K
153K
10^-1
10^-2
10^-2
10^0
10^2
10^4
10^6
f (Hz)

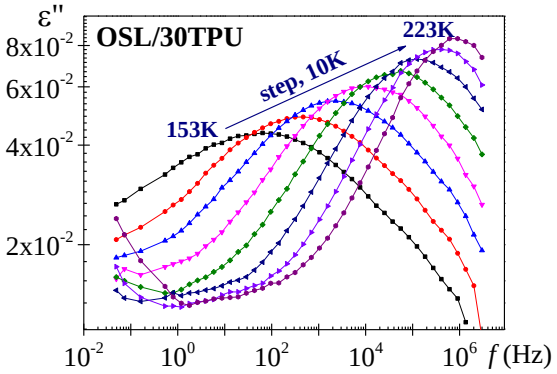
ε''
OSL/30TPU
223K
step, 10K
153K
8x10^-2
6x10^-2
4x10^-2
2x10^-2
10^-2
10^0
10^2
10^4
10^6
f (Hz)

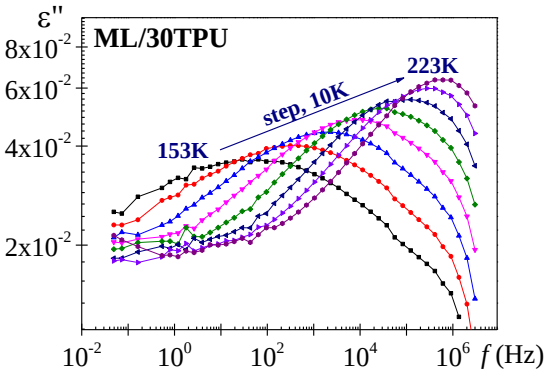
ε''
ML/30TPU
223K
step, 10K
153K
8x10^-2
6x10^-2
4x10^-2
2x10^-2
10^-2
10^0
10^2
10^4
10^6
f (Hz)

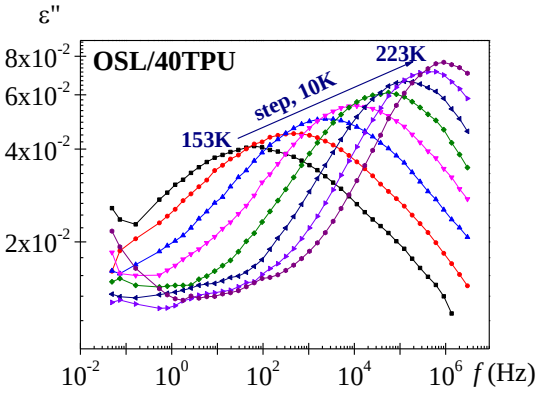
ε''
OSL/40TPU
223K
step, 10K
153K
8x10^-2
6x10^-2
4x10^-2
2x10^-2
10^-2
10^0
10^2
10^4
10^6
f (Hz)

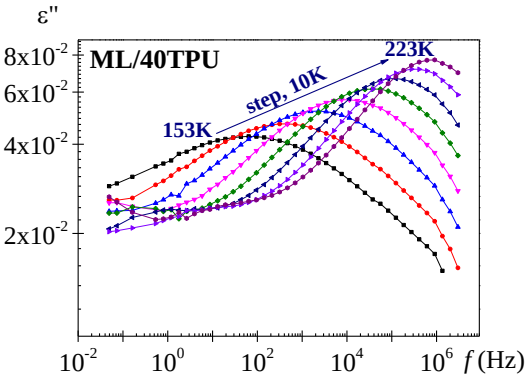
ε''
ML/40TPU
223K
step, 10K
153K
8x10^-2
6x10^-2
4x10^-2
2x10^-2
10^-2
10^0
10^2
10^4
10^6
f (Hz)

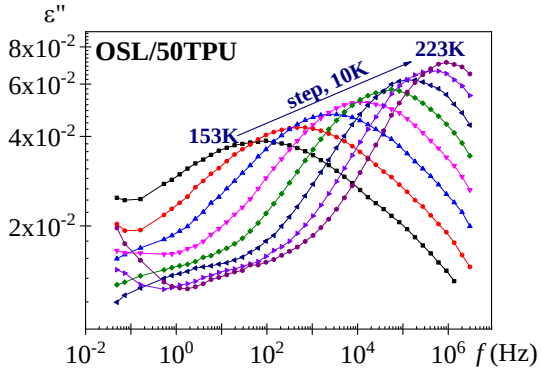
ε''
OSL/50TPU
223K
step, 10K
153K
8x10^-2
6x10^-2
4x10^-2
2x10^-2
10^-2
10^0
10^2
10^4
10^6
f (Hz)

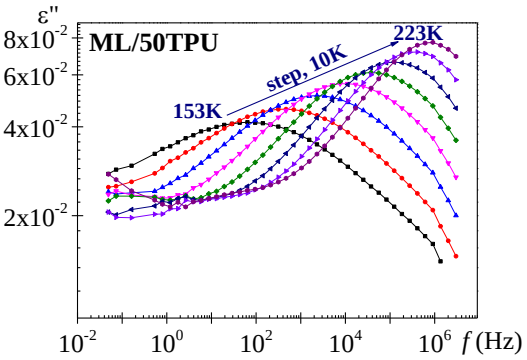
ε''
ML/50TPU
223K
step, 10K
153K
8x10^-2
6x10^-2
4x10^-2
2x10^-2
10^-2
10^0
10^2
10^4
10^6
f (Hz)

Fig. 7. Frequency dependence of the ε″ for TPU and lignin/*x*TPU blends (*x*=0, 30, 40, 50 and lignin = OSL and ML) between 153 K and 223 K.

The HN parameters of the low temperature process (β-relaxation) were determined at several temperatures from a multiple non-linear regression analysis of the experimental data. The four characterizing peak parameters (Δε, τ, a_{HN}, b_{HN}) were allowed to vary and the obtained values are summarized in Fig. 8, b_{HN} was equal to 1 in all cases as expected.

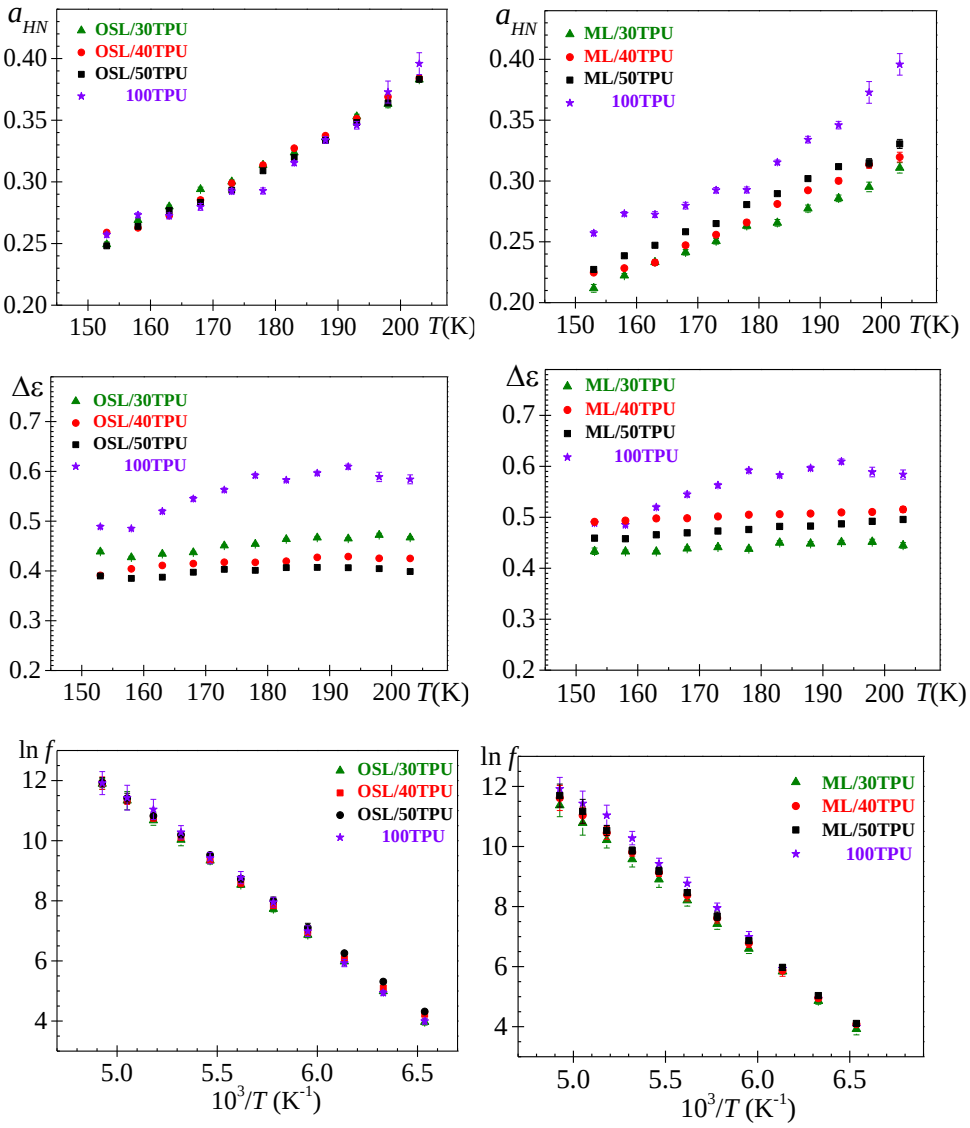

Fig. 8. Temperature dependence of the shape parameter a_{HN}, strength relaxation $\Delta\varepsilon$ and frequency of maximum ($\omega\tau = 1$, $\omega = 2\pi f$) for the low temperature dielectric process of TPU and lignin/*x*TPU blends.

Fig. 9 shows the lignin/*x*TPU ratio dependence of the obtained fit parameters at a specific temperature, 173 K. From both Figures it can be seen that the a_{HN} shape parameter value is hardly affected by the OSL incorporation, which indicates that the local environment of the relaxing groups was significantly unchanged. However, the a_{HN} shape parameter value is significantly reduced by the ML incorporation, pointing out that the local environment of the relaxing groups became more heterogeneous. This reduction is related to the relaxation broadening observed with the ML incorporation (see inset in Fig. 9a where, as an example, the normalized loss permittivity of lignin/50TPU blend at 173 K is plotted).

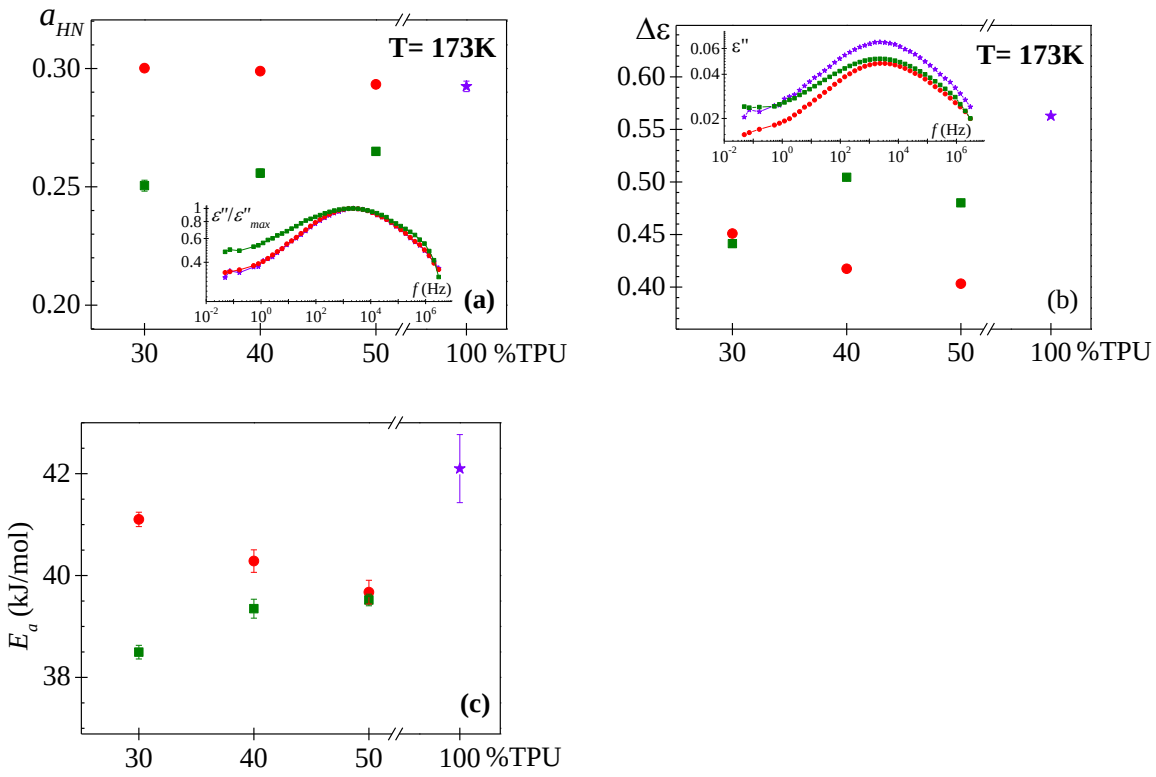

Fig. 9. Composition dependence of the a_{HN} (a), Δε (b), and activation energy (c) of low temperature dipolar process of TPU (violet star), OSL/*x*TPU (red circle) and ML/*x*TPU (green square) blends at 173K. Insets: frequency dependence of the loss permittivity (b) and this normalized plot (a) for lignin/50TPU at 173 K.

Regarding the dielectric relaxation strength, $\Delta\varepsilon$, a decrease is induced for the lignin (OSL or ML) presence, giving insights into the number of segments contributing to the β-relaxation process. Thus, for blends with 70% of lignin (30% TPU), both lignin types display similar behavior. However, for higher TPU contents (40%, 50%) some differences occur. Taking into account that this parameter is directly related to the dipolar moment, this relaxation behavior is in agreement with FTIR results of our previous work, which show strong interactions between both, lignin and TPU [27]. Whereas the OSL addition favors the H-bonding interactions with TPU (chemical interactions between the soft segment of TPU and lignin polymer chains), interestingly the ML addition inhibits the formation of H-bonding with TPU, as shown in our previous work [27]. Both lignins clearly reduce the mobility of TPU chains, with behavioral differences depending on the chemical nature of the associated interactions.

Finally, as is shown in Fig. 8, the dynamics of the β-relaxation process exhibited an Arrhenius temperature dependence. For OSL/*x*TPU blends no changes are observed upon compositional change while for ML/*x*TPU blends, the activation curves are not overlapped, especially at high temperatures, probably due to interactions between the ML chains. The activation energies (E_a) obtained from the slopes of the Arrhenius plots are shown in Fig. 9c as a function of the blend composition, where a decrease in the E_a values with the incorporation of both types of lignin is observed when comparing to the TPU sample. However, the dependence on the composition is

opposite for both lignins, *i.e.* E_a increases with the OSL content but decreases with the ML incorporation. This behavior is attributed to the different chemical structure of OSL and ML lignins, which controls the interactions with TPU.

From Fig. 3 and 4, it was shown that, as temperature increases, the dipolar processes associated with the glass transition temperature of the soft and hard segments of the TPU appear in the spectra. However, the definition is poor in the loss dielectric spectrum due to the presence of conductive processes, which are dominant at high temperatures and low frequencies. Therefore, in order to eliminate the masking effect produced by conductive processes and clarify the origin of responses, Fig. 10 shows the temperature dependence of the dielectric loss modulus at a frequency of 1 Hz, for both, pure TPU and lignin/40TPU blends (lignin = OSL and ML). Additionally, the equivalent mechanical modulus, E'', is represented for comparison. The process associated with the lignin T_g is better visualized in the case of the ML/40TPU.

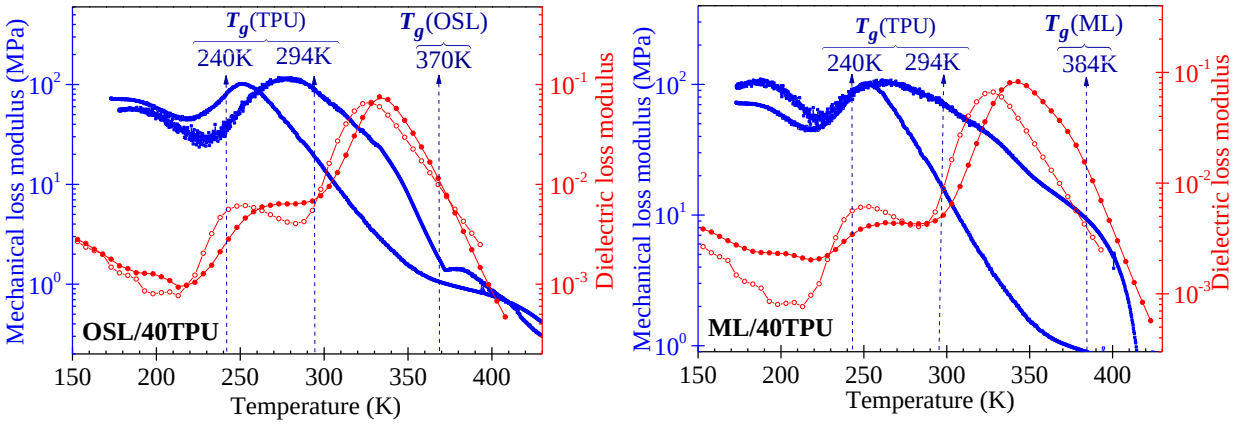

Fig. 10. Temperature dependence of the mechanical (left) and dielectric (right) loss modulus of TPU (open symbols) and lignin/40TPU (full symbols). The dashed lines mark the glass transition temperatures of the blend components evaluated by DSC.

Dielectric spectra at high temperatures are very complex, making the characterization of the segmental processes of pure components unfeasible. As expected for miscible or partially miscible polymer blends, Fig. 10 shows changes in position, broadness and intensity in the main segmental α-relaxation processes when compared with the pure components. These changes depend on the type of lignin and their different molecular structure. Thus, parameters such as initial branching degree, molecular weight and phenolic content determine the interactions within polymer blends of lignin and TPU.

Moreover, with the aim to visualize and characterize the ohmic conductivity, Fig. 11 shows the real part of the conductivity (left) and the imaginary part of the dielectric modulus (right). The ac conductivity was calculated from the dielectric permittivity according to the relationship $\sigma^*(\omega) = j\omega e_0 \varepsilon^*(\omega)$, where e_0 is the vacuum permittivity. As we can see, σ'_{ac} ($=\omega e_0 \varepsilon''$) changes drastically with composition and frequency [42]. At a constant temperature, the ac conductivity can be expressed by means of the ac universal law, as $\sigma_{ac}(\omega)=\sigma_{dc} + A\ \omega^s$ where σ_{dc} is the ac conductivity at the low frequency limit (value that is frequency independent) and A, s are temperature dependent parameters [43-45]. At high frequencies, as it is expected, σ'_{ac} increases linearly with increasing frequency [44]. For OSL/*x*TPU blends the dc conductivity values are between those of their constituents, OSL and TPU, increasing in value as the ratio OSL to TPU increases. According to our previous results [46] when the temperature increases the OSL sample reaches sufficient internal molecular mobility to form ring to ring crosslinks, thereby enhancing conductivity. On the other hand, for ML/*x*TPU blends dc conductivity values are lower than those of their constituents, with a large reduction as the ratio ML to TPU increases. It appears

that the ML lignin inhibits the hydrogen bonding interactions with the TPU chains promoting the separation of microphases of the hard and soft segments of the TPU. This phase separation is responsible for the MWS process observed in the middle of the conductivity spectra. The presence of the MWS process only in ML/*x*TPU blends is clearly visualized in loss dielectric modulus (see Fig. 11 right). We would like to emphasize that the significant reduction in the conductivity, as well as the better definition of the MWS process observed for the ML/30TPU blend, is related to both, the crosslinking produced between the ML chains as the temperature increases, and with the inhibition of the hydrogen bonding interactions with the TPU chains [46].

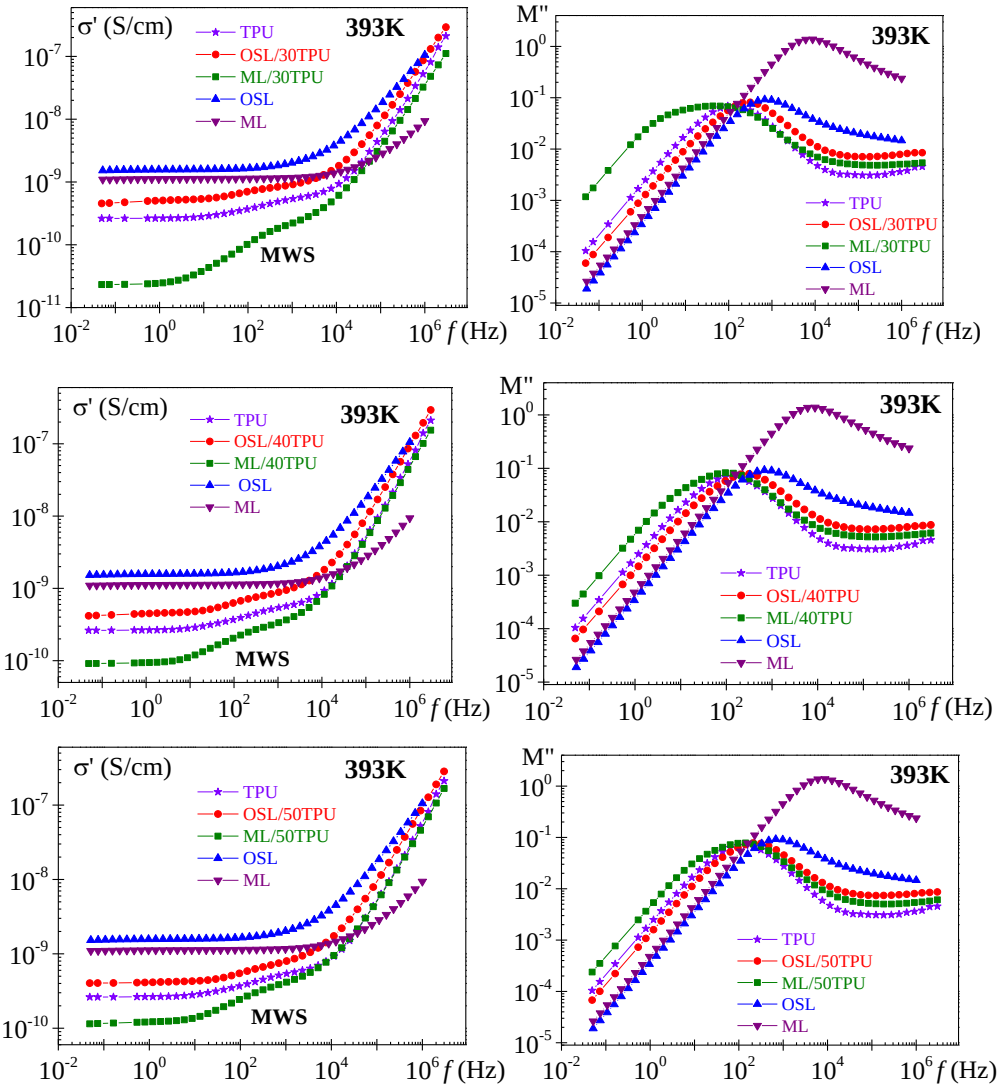

Fig. 11. Frequency dependence of the ac conductivity (left) and loss dielectric modulus (right) of TPU, OSL, ML and lignin/*x*TPU (*x*= 30, 40 and 50) at 393 K.

Fig. 12 shows the temperature dependence of the dc conductivity values obtained from extrapolation to low frequencies from the frequency dependence of σ'_{ac}. As we can observe this dependence is well defined by the Arrhenius equation, from which the conductive activation energy of the analyzed blends was evaluated. The obtained activation energy values are plotted in Fig. 13 as a function of the TPU composition. The tendency is the inverse to that observed in the energy barrier of the low temperature process. In this case, a reduction of the activation energy is observed with the increase of OSL lignin content in OSL/*x*TPU blends and an increase of the activation energy occurs when increasing ML lignin content in ML/*x*TPU blends. In the last case, ML/*x*TPU blends, this trend may be related to the increase in the cross-linking that takes place between ML molecular chains as temperature increases [46]. This structural change hinders electric transport, decreasing conductivity and increases the energy barrier associated with the process. Thus, the different nature of the interactions between TPU and the two lignins studied contributes to the differences in the electrical conductivity. For ML/*x*TPU blends it appears that segregation between hard and soft segments of TPU inhibits electric transport, while in OSL/*x*TPU blends conductivity processes are more favorable due to hydrogen bonding, lower branching degree and chain mobility which increases the electron mobility between polymer chains [33].

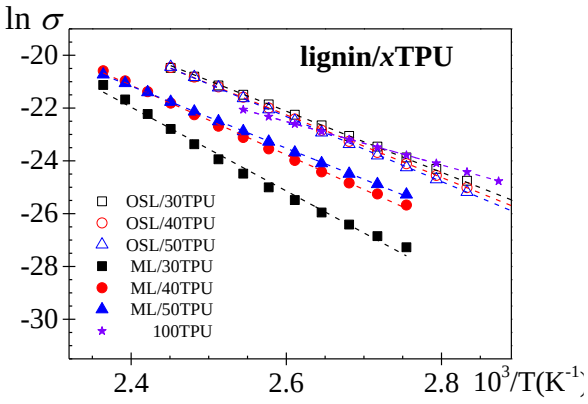

Fig. 12. Temperature dependence of the dc conductivity for the TPU and lignin/*x*TPU blends.

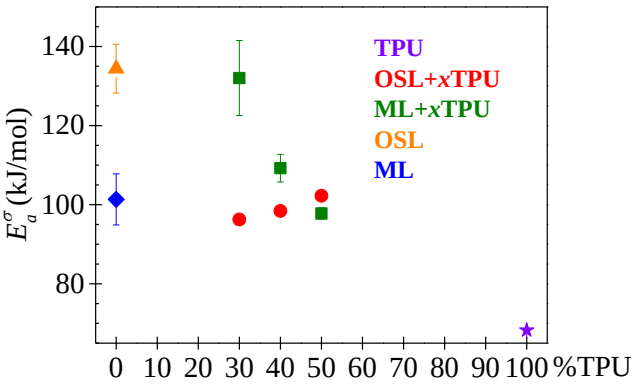

Fig. 13. Composition dependence of the energy barrier of ohmic conductive process for TPU (violet star), OSL (orange triangle), ML (blue diamond), OSL/*x*TPU (red circle) and ML/*x*TPU (green square).

4. Conclusion

We attribute differences in the molecular structure between ML and OSL lignins (branching degree, phenolic content and molecular weight) as determining factors that govern the interactions with TPU and ultimately the thermal/processing behavior of these blends.

Mechanical and dielectric spectra shown two relaxation processes associated with the chain mobility of the TPU chains, which are differently affected by the chemical nature of the lignin.

The presence of lignins suppresses the α-relaxation process in the blends compared to TPU and the local β-relaxation process was strongly influenced by the formation of intermolecular bonds.

For OSL blends, there is a strong coupling between both components of the blend through intermolecular hydrogen bonding which leads to an indiscernible glass transition. Chemical linkages between OSL and TPU play a dominant role in suppressing α-relaxation processes and in decreasing the activation energy of localized β-relaxation processes of the blends.

For ML blends, the dielectric relaxation strength of the local relaxation process, $\Delta\varepsilon_\beta$, was proportional to the TPU content, which suggested that blending and intermolecular interactions did not modify the local intramolecular motion.

In addition, changes are observed in the conductivity behavior of both blends due to the differing molecular interactions between lignin type and TPU chains.

Taken overall, these results demonstrate that the dielectric behavior of these two lignins blended with bio-based TPU, follow very different paths at the molecular level. In both cases, on heating, there is a competition between thermodynamic and kinetic factors, as fluidity initially increases facilitating a reaction, however, reactions follow different pathways leading to structurally different end products.

Acknowledgment

M. Carsí and M.J. Sanchis thank the Spanish Ministerio de Economia y Competitividad (RTI2018-093711-B-I00) for partial financial help. M. Culebras and M. N Collins acknowledge received funding from the Bio-Based Industries Joint Undertaking under the European Union's Horizon 2020 research and innovation programme under grant agreement no. 720707.

References

[1] M.F. Ashby, Materials and sustainable development, first ed., Butterworth-Heinemann, 2015.

[2] L.Y. Ljungberg, Materials selection and design for development of sustainable products, Materials & Design 28 (2) (2007) 466-479.

[3] M.N. Belgacem, A. Gandini, Lignins as Components of Macromolecular Materials, in: M.N. Belgacem, A. Gandini (Eds.), Monomers, polymers and composites from renewable resources, Elsevier, 2008, pp 243−271.

[4] Z. Yunqing, C. Romain, C.K. Williams, Sustainable polymers from renewable resources, Nature 540 (7633) (2016) 354-362.

[5] J.-P. Lange, Sustainable development: efficiency and recycling in chemicals manufacturing, Green Chemistry 4 (6) (2002) 546-550.

[6] S. Dutta, J. Kim, Y. Ide, J. Ho Kim, Md. S. A. Hossain, Y. Bando, Y. Yamauchi, K. C.-W. Wu., 3D network of cellulose-based energy storage devices and related emerging applications, Materials Horizons 4 (2017) 522-545.

[7] C-T Chen, C. Van Nguyen, Z-Y. Wang, Y. Bando, Y. Yamauchi, M. Tareq, S. Bazziz, A. Fatehmulla, W. A. Farooq, T. Yoshikawa, T. Masuda, K. C.-W. Wu, Hydrogen Peroxide

Assisted Selective Oxidation of 5-Hydroxymethylfurfural in Water under Mild Conditions. ChemCatChem 10 (2018) 361-365.

[8] Y-T. Liao, B. M. Matsagar, K. C.-W. Wu, Metal-Organic Frameworks (MOFs) Derived Effective Solid Catalysts for the Valorization Lignocellulosic Biomass, ACS Sustainable Chemistry & Engineering 6(11) (2018) 13628-13643.

[9] B. M. Matsagar, S. A. Hossain, T. Islam, H. R. Alamri, Z. A. Alothman, Y. Yamauchi, P. L. Dhepe, K. C.-W. Wu, Direct Production of Furfural in One-pot Fashion from Raw Biomass Using Brønsted Acidic Ionic Liquids, Scientific Reports 7 (2017) 13508.

[10] C. Van Nguyen, D. Lewis, W-H. Chen, H-W. Huang, Z. A. ALOthman, Y. Yamauchi, K. C.-W. Wu, Combined treatments for producing 5-hydroxymethylfurfural (HMF) from lignocellulosic biomass, Catalysis Today 278 (2016) 344-349.

[11] R.A. Sheldon, Green and sustainable manufacture of chemicals from biomass: state of the art, Green Chemistry 16 (3) (2014) 950-96.

[12] J. Nyoo Putro, F. Edi Soetaredjo, S-Y. Lin, Y-H Ju, S. Ismadji, Pretreatment and conversion of lignocellulose biomass into valuable chemicals, RSC Advances 6 (52) (2016) 46834-46852.

[13] A.J. Ragauskas, G.T. Beckham, M.J. Biddy, R. Chandra, F. Chen, M.F. Davis, B.H. Davison, R.A. Dixon, P. Gilna, M. Keller, P. Langan, A.K. Naskar, J.N. Saddler, T.J. Tschaplinski, G.A. Tuskan, C.E. Wyman, Lignin valorization: improving lignin processing in the biorefinery, Science 344 (6185) (2014) 1246843.

[14] K. Sriranga, L. Akawi, M. Moo-Young, C.P. Chou, Towards Sustainable Production of Clean Energy Carriers from Biomass Resources, Applied energy 100 (2012) 172-186.

[15] M.N. Satheesh Kumar, A.K. Mohanty, L. Erickson, M. Misra, Lignin and Its Applications with Polymers, Journal of Biobased Materials and Bioenergy 3(1) (2009) 1-24.

[16] J.F. Kadla, S. Kubo, R.A. Venditti, R.D. Gilbert, Novel Hollow Core Fibers Prepared from Lignin Polypropylene Blends, Journal of Applied Polymer Science 85 (2002) 1353–1355.

[17] J.L. White, S.H. Bumm, Polymer blend compounding and processing, in: A.I. Isayev (Ed.), Encyclopedia of Polymer Blends: Volume 2: Processing, Wiley-VCH, 2011, pp. 1–26.

[18] S. Thomas, D. Durand, C. Chassenieux, P. Jyotishkumar, Handbook of Biopolymer-Based Materials from Blends and Composites to Gels and Complex Networks, first ed., Ed. Wiley-VCH, 2013.

[19] F. Erik, F. Hermanutz, M.R. Buchmeiser, Carbon Fibers: Precursors, Manufacturing, and Properties, Macromolecular materials and engineering 297 (6) (2012) 493-501.

[20] J.F Kadla, S Kubo, R.A Venditti, R.D Gilbert, A.L. Compere, W Griffith, Lignin-based carbon fibers for composite fiber applications, Carbon 40 (15) (2002) 2913-2920.

[21] R. Rinaldi, R. Jastrzebski, M.T. Clough, J. Ralph, M. Kennema, P.C.A. Bruijnincx, B.M. Weckhuysen, Paving the Way for Lignin Valorisation: Recent Advances in Bioengineering, Biorefining and Catalysis, Angew. Chem. Int. Ed. Engl. 55 (29) (2016) 8164-8215.

[22] S. Kubo, J.F. Kadla, Poly(Ethylene Oxide)/Organosolv Lignin Blends: Relationship between Thermal Properties, Chemical Structure, and Blend Behavior, Macromolecules 37 (18) (2004) 6904-6911.

[23] D. Kun, B. Pukánszky, Polymer/lignin blends: Interactions, properties, applications, European Polymer Journal 93 (2017) 618-641.

[24] H. Jeong, J. Park, S. Kim, J. Lee, J.W. Cho, Use of acetylated softwood kraft lignin as filler in synthetic polymers, Fibers and Polymers 13 (2012) 1310-1318.

[25] C. Liu, C. Xiao, H. Liang, Properties and structure of PVP–lignin "blend films", J. Appl. Polym. Sci. 95 (2005) 1405-1411.

[26] V. Kumar Thakur, M. Kumari Thakur, P. Raghavan, M.R. Kessler, Progress in Green Polymer Composites from Lignin for Multifunctional Applications: A Review, ACS Sustainable Chemistry & Engineering 2 (5) (2014) 1072-1092.

[27] M. Culebras, A. Beaucamp, Y. Wang, M.M. Clauss, E. Frank, M.N. Collins, Biobased Structurally Compatible Polymer Blends Based on Lignin and Thermoplastic Elastomer Polyurethane as Carbon Fiber Precursors, ACS Sustainable Chem. Eng. 6 (2018) 8816−8825.

[28] S. Zhang, P.C. Painter, J. Runt, Coupling of Component Segmental Relaxations in a Polymer Blend Containing Intermolecular Hydrogen Bonds, Macromolecules 35 (2002) 8478-8487.

[29] K.A. Masser, H. Zhao, P.C. Painter, J. Runt, Macromolecules 43 (21) (2010) 9004–9013.

[30] A. Schönhals, F. Kremer, Broadband dielectric spectroscopy, Springer-Verlag Berlin Heidelberg New York, 2003.

[31] S. Thomas, Y. Grohens, P. Jyotishkumar, Characterization of Polymer Blends. Miscibility, Morphology and Interfaces, Wiley-VCH Verlag GmbH & Co. KGaA, 2015.

[32] P. Ortiz-Serna, M. Carsí, B. Redondo-Foj, M.J. Sanchis, M Culebras, C.M. Gómez, A. Cantarero, Thermal and Dielectric Properties of Polycarbonatediol Polyurethane, J. Appl. Polym. Sci. 132 (22) (2015) 42007 (8pp).

[33] H. Hatakeyama, H. Matsumura, T. Hatakeyama, Glass transition and thermal degradation of rigid polyurethane foams derived from castor oil-molasses polyols, Journal of thermal analysis and calorimetry 111 (2013) 1545–1552.

[34] J.C. Maxwell, Electricity and Magnetism, Clarendon Press, Oxford, 1893.

[35] K.W. Wagner, Explanation of the dielectric after-effects on the basis of Maxwell's ideas, Archiv für Elektrotechnik 2 (1914) 371–387.

[36] R.W. Sillars, Properties of a Dielectric Containing Semi-Conducting Particles of Various Shapes, J. Inst. Electr. Eng. 80 (1937) 378–394.

[37] P. Ben Ishai, M.S Talary, A. Caduff, E. Levy, Y. Feldman, Electrode polarization in dielectric measurements: a review, Meas. Sci. Technol. 24 (2013) 102001 (21pp).

[38] I.M. Hodge, K.L. Ngai and C.T. Moynihan, Comments on the electric modulus function, Journal of Non-Crystalline Solids 351 (2005) 104–115.

[39] S. Havriliak, S. Negami, A complex plane representation of dielectric and mechanical relaxation processes in some polymers, Polymer 8 (4) (1967) 161-210.

[40] S. Havriliak, S.Negami, A complex plane analysis of α-dispersions in some polymer systems, Journal of Polymer Science Part C: Polymer Symposia 14 (1966) 99-117.

[41] S. Havriliak, S. Negami, Dielectric and Mechanical Relaxation in Materials, Hanser: Munich, 1997.

[42] M. Carsí, M.J. Sanchis, P. Ortiz-Serna, B. Redondo-Foj, R. Díaz-Calleja, E. Riande, Conductivity And Time-Temperature Correspondence In Polar Viscoelastic Liquids, Macromolecules 46 (2013) 3167−3175.

[43] A.K. Jonscher, Universal Relaxation Law: A Sequel to Dielectric Relaxation in Solids, Chelsea Dielectrics Press, London, 1996.

[44] J.C. Dyre, T.B. Schrøder, Universality of ac conduction in disordered solids, Reviews of Modern Physics 72 (2000) 873–892.

[45] J.C. Dyre, The random free-energy barrier model for ac conduction in disordered solids, Journal of Applied Physics 64 (1988) 2456–2468.

[46] M. Culebras, M.J. Sanchis, A. Beaucamp, M. Carsí, B.K. Kandola, A.R. Horrocks, G. Panzetti, C. Birkinshaw, M.N. Collins, Understanding the thermal and dielectric response of organosolv and modified kraft lignin as a carbon fibre precursor, Green Chemistry 20 (2018) 4461-4472.